STUDY OF RADIATIVE HEAT TRANSFER IN A FLUIDIZED BED

A. I. Il'chenko, V. S. Pikashov, and K. E. Makhorin

Inzhenerno-Fizicheskii Zhurnal, Vol. 14, No. 4, pp. 602–608, 1968

UDC 536.3:536.246

The radiative component can be measured with the aid of two radiometer probes. Experimental data for bed temperatures up to 1700° K are presented as functions of the principal hydrodynamic and thermal parameters.

The effect of the radiative component on heat transfer in a fluidized bed has been much discussed [1–8], but, as far as is known, none of the theories has been verified experimentally.

This paper describes a method of determining experimentally the radiative component using two radiometer probes. The technique is similar to that employed to investigate flames.

In the case of flames there are several experimental methods of separating the radiative and convective heat transfer components [10]. Two of these are applicable to a fluidized bed: the method employing two radiometers with different detecting-surface absorptivities and the method based on two radiometers, one of which registers the total heat flux and the other the radiant flux [11]. The first method requires that the absorptivities differ by several times and remain constant during the experiment. This can be achieved with two metal surfaces, one of which is polished and the other blackened. However, because of the abrasive action of the fluidized bed particles the absorptivities rapidly approach each other.

Accordingly, we selected the second method, which does not suffer from the disadvantages of the first.

In our experiments the radiant heat flux was registered by a narrow-angle total-radiation radiometer probe designed at the Gas Institute AS Ukrainian SSR (the use of a narrow-angle rather than a hemispherical radiometer in a fluidized bed is legitimate since for such systems Lambert's law is fully observed). The probe (Fig. 1) consists of a plane thermoelectric detector 1 [12] mounted on a copper plug 2. The plug and detector are secured to the bottom of a hollow thick-walled copper cylinder 3, which is placed in a water-cooled jacket 4. The probe is designed to be highly stable, and the accuracy of the measurements is independent of the ambient temperature.

To prevent particles from entering the instrument cavity, the latter is separated from the ambient medium by a thin disk of quartz optical glass 5. The spectral transmittance of the quartz is quite high over a broad range of wavelengths. The glass is held tightly against the instrument housing by a threaded upper ring 6, and thanks to the large area of contact with the water-cooled surface its temperature does not exceed 100–200° C. This keeps the optical properties constant and prevents crystallization of the quartz, which could otherwise occur at high temperatures [13].

The probe was calibrated against a simulated ideal blackbody in the temperature range from 500 to 1300° C. After this the graph (Fig. 1)

$$E_{rad} = f(q_0) = f(\sigma T_{bb}^4). \quad (1)$$

was constructed.

The calibration was first carried out without the quartz glass (a) and then with optically transparent quartz (b) with a polished surface. In both cases a linear $E = f(q_0)$ relation was obtained. In the bed, owing to the intense friction of the particles against the glass its surface was dulled. Accordingly, after the experi-

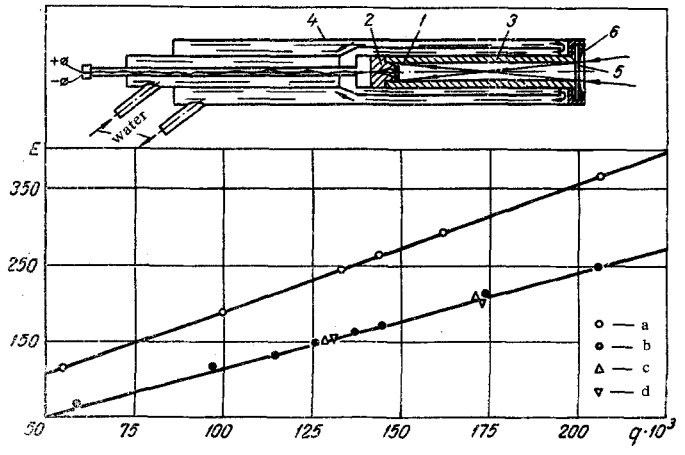

Fig. 1. Diagram of the radiometer probe and calibration curves (for notation see text).

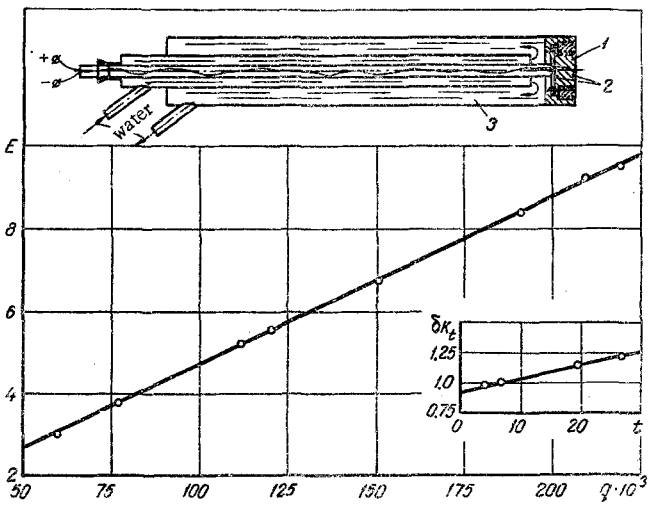

Fig. 2. Diagram of the total heat flux probe and calibration curve (for notation see text).

ment was over we carried out a second calibration of the probe for three glasses: 1) with a polished surface (b), 2) lightly scratched after 12 hours operation in a bed of 1–1.5-mm MgO and SiO_2 particles (c), and 3) deeply scratched after 12 hours operation in a bed of 1.5–2-mm corundum particles (d). Within the limits of experimental error the points lay on the same straight line, which indicates constancy of the transmittance. This is attributable obviously to the fact that the surface of the glass, originally flat and uniform, was replaced by a system of small surfaces randomly distributed but without effect on the transmission properties, so that for diffuse radiation the over-all surface produces the same effect.

As the radiometer for registering the total heat flux we used an end-face probe designed at the All-Union Scientific Research Institute for Metallurgical Thermal Engineering [12] (Fig. 2). The total heat flux is registered by the detecting surface 1, one side of which is turned toward the measured medium, while the other is water-cooled. In this case the heat flux is proportional to the difference between the temperatures of the outer and inner surfaces of the detector, measured by a differential thermocouple 2. The heat-absorbing surface of the detector was made rough, so that there was no change in surface microstructure before and after the experiments.

The probe was similarly calibrated before and after the experiments on a black body with respect to radiant heat flux. The heat transfer from the air to the detector due to natural convection was neglected. A disadvantage of this type of probe is the effect of the temperature of the cooling water on the accuracy of the measurements [12]. Accordingly, the jacket 3 was insulated as thoroughly as possible and, moreover, a correction coefficient δK_t was determined as a function of the temperature of the cooling water. The results of the calibration are presented in Fig. 2. The radiant heat flux was calculated from the graph or from the formula

$$q_{rad} = K_{rad} E_{rad}. \quad (2)$$

Similarly, the total heat flux

$$q_{total} = K_{total} \delta K_t E_{total}. \quad (3)$$

Since the total heat flux probe was calibrated with respect to the radiant flux, while the total heat flux also includes a conductive component, at a detector absorptivity $a_m < 1$ the measured conductive component will be too high. Blackening the surface proved impossible owing to the intense abrasion. Accordingly, in the calculations for the convective-conductive component we introduced a correction for the detector absorptivity.

Table 1

Characteristics of the Fine-Grained Materials Used in the Experiments

Parameter	Material				
	river sand	chamotte	fused magnesite	corundum	zirconium dioxide
Fraction, mm	1 — 1.5	1 — 1.5	1 — 1.5	1.5 — 2	0.20 — 1.0
Equivalent diameter	1	1.15	1.07	1.75	0.57
Particle shape	rounded	sharp-angled	sharp-angled lamellar	spherical	sharp-angled lamellar

$$q_{total} = \frac{q_{cc}}{a_m} + q_{rad}. \quad (4)$$

From Eqs. (3) and (4)

$$q_{cc} = a_m(K_{total}\delta K_t E_{total} - q_{rad}). \quad (5)$$

The value of a_m, which was determined experimentally, is constant for radiator temperatures of 900–1300° C and equal to 0.832. In the experiments the temperature of the outer surface of the detector remained within the limits 60–120° C.

The experiments were conducted on the apparatus described in [14]. The probes were introduced into the heating chamber through lateral openings 120 mm from the distributor and projected 50 mm inside. The temperature of the bed was measured with a platinum thermocouple in the same plane as the probes. As the gas distributor we used a high-alumina porous plate which made it possible to ignite natural gas both in the bed and beneath the distributor. Bed temperatures above 1300° K were obtained by igniting the gas in the bed. In all cases the thickness of the dense bed was equal to the diameter of the heating chamber (220 mm). The results of the measurements were calculated from Eqs. (2) and (5).

The characteristics of the particles used in the experiments are presented in Table 1. The equivalent diameter of the particles was determined from Leva's formula [6].

The dependence of the total heat flux on bed temperature (Fig. 3a) is linear for all the particle sizes investigated. Only for corundum is a deviation from linearity observed, starting from 1500° K.

In the experiments with river sand the data lay on the same straight line as the experimental points for sharp-angled chamotte particles of the same size. This was also observed in investigating the heat transfer to individual tubes for three materials of the same fraction: fused magnesite, chamotte, and sand. The thermophysical characteristics of river sand and chamotte differ only slightly.

This indicates that at high temperatures the particle shape does not play such a decisive role as in conductive heat transfer. There are data [9, 14] showing that the heat transfer coefficients are different for particles of the same fraction but different shape. The reason for this must evidently be sought not in the shape of the particles themselves but primarily in the different percentage composition with respect to particle size within the fraction. This is especially important for fine fractions (<0.8 mm), where the effect of particle size on heat transfer rate is stronger.

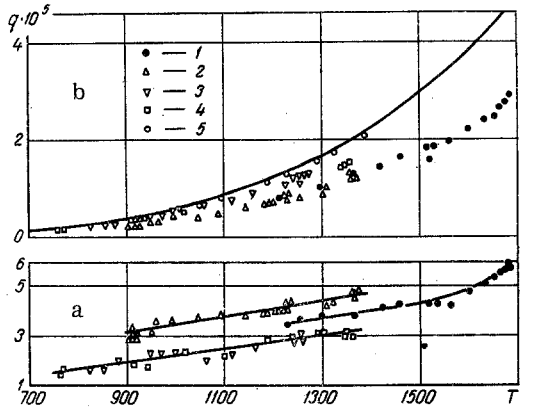

Fig. 3. Total (a) and radiant (b) heat fluxes q (W/m²) as a function of temperature T (°K) for various bed materials: 1) corundum, 2) zirconium dioxide, 3) river sand, 4) chamotte, 5) fused magnesite.

In our experiments the flow velocity was not observed to affect either the total or the radiant heat flux. Table 2 presents the results obtained for particles of zirconium dioxide at a bed temperature of 1223° K. Within the limits of experimental error the heat flux remains constant for all the flow velocities investigated.

The effect of bed temperature on the incident radiant flux measured by the radiometer 1 is presented in Fig. 3b. The solid curve represents the limiting value of the radiant flux calculated for an ideal black body. All the experimental points lie beneath the curve. Moreover, as the temperature rises, the extent to which the actual flux lags behind the calculated flux increases for all the materials without exception. For example, whereas the measured flux for ZrO_2 at 903° K is 80% of the calculated value, at 1308° K it is only 59%. However, the lag is different for different materials. The experimental points for sand and chamotte particles are close to the calculated curve up to a temperature of 1000° K and for fused magnesite particles up to 1400° K.

We conducted experiments to determine the degree of cooling of the particles on individual water-cooled tubes 30 and 10 mm in diameter. The outer surface of the tube was kept at a temperature of 330–340° K. The temperature gradient between the bed and the sur-

Table 2

Effect of Flow Velocity of Fluidizing Agent on the Heat Flux in a Fluidized Bed of Zirconium Dioxide Particles

Heat flux W/m²	Flow velocity, m/sec							
	0.48	0.633	0.71	0.761	0.78	0.99	1.045	1.26
q_{rad}	83800	88100	76000	80600	78500	78000	78900	80000
q_{total}	400000	414000	408000	404000	401000	397000	404000	400000

Remark. Velocity at onset of fluidization of zirconium dioxide particles 0.38 m/sec.

face of the tube was measured with a chromel-alumel thermocouple with thermoelectrodes 0.1 mm in diameter. To avoid disrupting the hydrodynamics of the

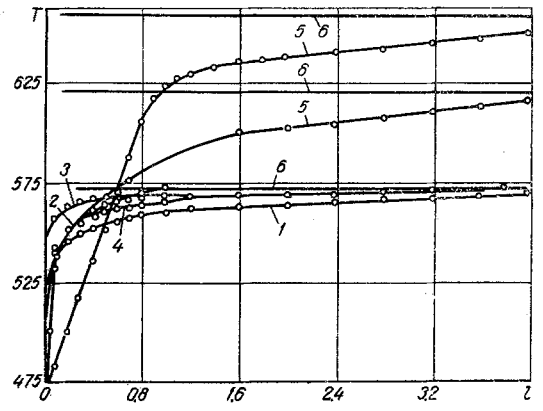

Fig. 4. Temperature gradient between fluidized bed and 30-mm water-cooled tube for various materials and fractions: *l*) distance from tube surface, mm; T) temperature, °K; 1) sand, 1–1.5 mm; 2) sand, 0.25–0.5 mm; 3) chamotte, 0.2–2 mm; 4) chamotte, 1–1.5 mm; 5) chamotte, 2–5 mm; 6) temperature of bed core.

particle flow and of the influx of heat to the thermocouple button (junction diameter 0.2 mm) over the thermal electrodes, the thermocouple was mounted between the burners. The distance between the thermocouple button and the surface of the tube was measured with a micrometer screw. The results of the measurements are presented in Fig. 4, from which it is clear that for all the particles investigated the thermocouple began to register the temperature of the main body of the bed at a distance of not more than one particle diameter, for example, for chamotte particles of the fraction 2–5 mm at a distance of 5 mm. In the initial position the thermocouple was placed close up against the tube. In spite of being in contact with the cold surface, it registered a temperature greatly exceeding the temperature of the tube. As the thermocouple moved 0.1 mm away from the surface, it was possible to observe a temperature jump, which was the sharper, the finer the particle. Obviously, only the first row is cooled and that only slightly, but enough to affect the radiant heat flux. The temperature gradient at a tube 10 mm in diameter is similar in form. Thus, the deviation of the actual radiant flux from the calculated value may be attributable to two simultaneously acting factors: cooling of the particles at the heated surface and the fact that the emissivity of the bed is different from 1 [15]. The relative influence of these factors remains to be determined.

NOTATION

E_{rad} and E_{total} are the emf's obtained respectively from measurements made with the radiant and total heat flux probes, mV; σ is the blackbody temperature in calibrating the probes, °K; q_0 is the blackbody radiation factor, W/m^2 · deg^4; T_{bb} is the blackbody heat flux, W/m^2; a_m is the absorptivity of metal detector surface (dimensionless); q_{rad}, q_{total}, and q_{cc} are the measured specific heat fluxes: radiant, total, and convective-conductive, respectively, W/m^2; K_{total} and K_{rad} are the calibration coefficients of total and radiant heat flux probes, respectively, W/m^2 · V; δK_t is the correction for cooling water temperature.

REFERENCES

1. S. S. Zabrodskii, Hydrodynamics and Heat Transfer in a Fluidized Bed [in Russian], Gosenergoizdat, 1963.

2. L. Jolley, Fuel, **28**, no. 5, 1949.

3. S. S. Zabrodskii, Heat and Mass Transfer in Disperse Systems [in Russian], Iz-vo Nauka i tekhnika, Minsk, p. 58, 1965.

4. A. I. Tamarin and V. D. Dunskii, Heat and Mass Transfer in Disperse Systems [in Russian], Iz-vo Nauka i tekhnika, Minsk, p. 58, 1965.

5. Fudzisige Kharauaki, Koge kagaku dzassi, Koduo Kadaki. Zasshi, J. Chem. Japan Industr. Chem. Soc., **67**, no. 9, 1329–1336, 1964.

6. M. Leva, Fluidization [Russian translation], Gostoptekhizdat, 1964.

7. A. P. Baskakov, G. K. Malinov, and Yu. M. Goldobin, Proc. Donetsk Conf. on High-Temperature Endothermic Processes in Fluidized Beds [in Russian], Donetsk, 1966.

8. M. A. Glinkov and V. V. Belousov, Izv. VUZ. Chernaya metallurgiya, no. 7, 1966.

9. D. G. Traber, V. B. Sarki, and I. P. Mukhlenov, ZhPKh, **33**, no. 10, 1960.

10. V. N. Adrianov, Radiative and Convective Heat Transfer [in Russian], Iz-vo AN SSSR, Moscow, 1960.

11. S. S. Filimonov, B. A. Khrustalev, and V. N. Adrianov, Convective and Radiative Heat Transfer [in Russian], Iz-vo AN SSSR, Moscow, 1960.

12. O. A. Gerashchenko and V. G. Fedorov, Heat-Engineering Experimental Technique [in Russian], Iz-vo Naukova dumka, Kiev, 1964.

13. E. M. Voronkova, B. N. Grechushnikov, G. I. Distler, and I. P. Petrov, Optical Materials for Infrared Technology [in Russian], Iz-vo Nauka, Moscow, 1965.

14. N. V. Kharchenko and K. E. Makhorin, IFZh, **7**, no. 5, 1964.

15. G. K. Rubtsov and N. I. Syromyatnikov, Izv. VUZ. Energetika, no. 5, 1963.

23 August 1967

Gas Institute AS UkrSSR, Kiev